Supporting Information

for

Exploring the Effects of Glyco-copolymer Architectures on the Solution Self-assembly of Amphiphilic Thermoresponsive Linear, Star, and Cyclic Polymers

Naoki Ozawa,[1] Ji Ha Lee,[2] Isamu Akiba,[3] and Tomoki Nishimura[1] *

[1] Department of Chemistry and Materials, Faculty of Textile Science and Technology,

Shinshu University, 3-15-1, Tokida, Ueda, Nagano 386-8567, Japan

[2] Chemical Engineering Program, Graduate School of Advanced Science and Engineering,

Hiroshima University, 1-4-1 Kagamiyama, Higashi-Hiroshima 739-8527, Japan

[3] Department of Chemistry and Biochemistry, University of Kitakyushu,

1-1 Hibikino, Kitakyushu, Fukuoka 808-0135, Japan

E-mail: nishimura_tomoki@shinshu-u.ac.jp

Materials

Materials for the synthesis of alkyne functionalized maltopentaose

Maltopentaose (purity > 95.0%) and acetic anhydride (purity > 97.0%) were purchased from Wako. Propargyl amine (purity > 97.0%) was purchased from TCI and used as received.

Materials for the synthesis of alkyne functionalized cycloamylose

5-Hexynoic acid (purity > 96.0%) and *N*,*N*-dimethyl-4-aminopyridine (DMAP; purity > 99.0%) were purchased from TCI and used as received. Cycloamylose (M_p(MALDI) = 4.2 × 10^3 g mol^{-1}; **Fig. S1**) and dicyclohexyl carbodiimide (DCC; purity > 97.0%), dimethyl sulfoxide (DMSO; super dehydrated for organic synthesis), *N*,*N*-dimethylformamide (DMF) were purchased from Wako. DMSO was used after drying over activated molecular sieves (4 Å) overnight and purging with argon prior to use.

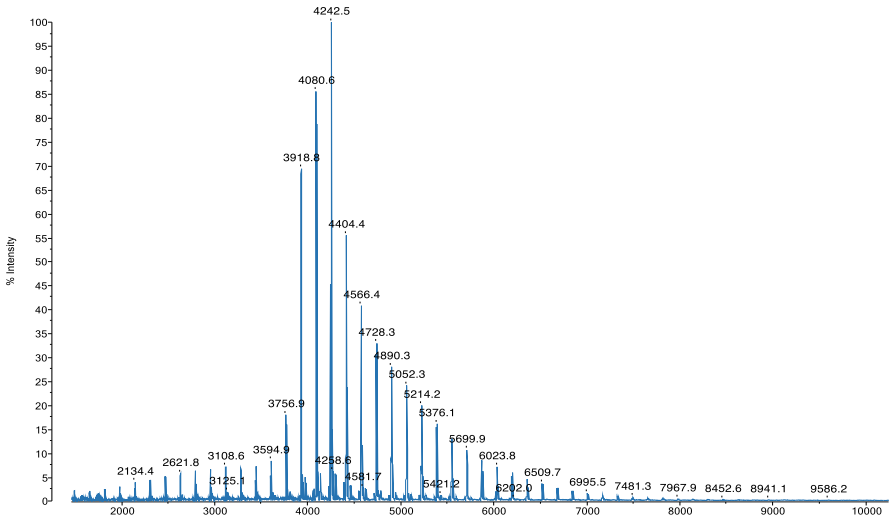

Fig. S1 MALDI-TOF mass spectrum of cycloamylose

Materials for the synthesis of azide-functionalized PPO (N_3-PPO) by end group substitution

Poly(propylene oxide) monobutyl ether (M_n = 1.0 × 10^3 g mol^{-1}), poly(propylene oxide) (M_n = 2.0 × 10^3 g mol^{-1}), P_4-t-Bu solution in hexane (purity > 99.0%) and Amberlite® (strongly acidic, hydrogen form) were purchased from Sigma-Aldrich and used as received. Methanesulfonyl chloride (purity > 99.0%), propylene oxide (PO; purity > 99.0%), 6-Bromo-1-hexanol (purity = 98.0%), 1,2,3,4-tetrahydronaphthalene (tetralin; purity > 98.0%), and acetic acid (AcOH; purity > 99.5%) were purchased from TCI and used as received. Sodium azide (purity = 98.0%), *N*,*N*-dimethylformamide (DMF), sodium azide, sodium sulfate (purity = 98%), *N*,*N*-dimethylformamide (DMF; super dehydrated for organic synthesis), and toluene (super dehydrated for organic synthesis) were purchased from Wako. Tetralin, DMF, and toluene were used after drying over activated molecular sieves (4 Å), and AcOH was used after drying over sodium sulfate overnight and purging with argon prior to use.

Materials for the synthesis of the amphiphilic polymers

N,*N*,*N*',*N*'',*N*''-pentamethyldiethylenetriamine (PMDETA; purity > 95.0%) was purchased from TCI and drying over sodium sulfate overnight and purging with argon prior to use. Copper bromide (CuBr; purity = 99.999%) was purchased from Sigma-Aldrich and used as received.

Materials for the acetylation of the cycloamylose and graft polymers

Acetic anhydride (purity > 97%) was purchased from Wako and used as received. *N*,*N*-dimethyl-4-aminopyridine (DMAP; purity > 99.0%) were purchased from TCI and used as received.

Synthesis

NMR spectroscopy

^{1}H NMR spectra were recorded in deuterated oxide (D_2O), methanol-d_4 (CD_3OD), chloroform-*d*, or dimethylsulfoxide (DMSO)-d_6/D_2O (9:1, v/v) using a Bruker Avance NEO 400 OneBay 400 MHz spectrometer. Chemical shifts (δ) are expressed in parts per million (ppm) and reported relative to tetramethylsilane (TMS; 0 ppm) as the internal standard.

Matrix assisted laser desorption/ionization mass spectrometry (MALDI-TOF-MS)

MALDI-TOF-MS spectrum of cycloamylose was measured on a Shimadzu MALDI-8020 mass spectrometer. 2, 5-dihydroxybenzoid acid was used as the matrix.

Size-exclusion chromatography (SEC)

The molecular weight distribution (MWD) curves, number-average molecular weights (M_n), and polymer dispersity indices ($Đ_M$) of the azide functionalized PPOs were measured via a SEC system (JASCO) equipped with refractive index detector in DMF containing 10 mM LiBr at 40 °C (flow rate = 0.35 mL min^{-1}) using two linear-type polystyrene gel columns (TOSOH TSKgel SuperHM-M; exclusion limit: 4×10^6 g mol^{-1}; particle size: 3 μm; pore size: N/A; 6.0 mm i.d. × 15 cm). The columns were calibrated against 12 poly(ethylene oxide) standards (PSS: $M_p = 2.38 \times 10^2$–9.69×10^5 g mol^{-1}; $Đ_M$(SEC) = 1.00–1.31) and 12 poly(methyl methacrylate) standards (PSS: $M_p = 8.00 \times 10^2$–2.20×10^6 g mol^{-1}; $Đ_M$(SEC) = 1.04–1.22).

Synthesis of the alkyne functionalized maltopentaose.

The alkyne functionalized maltopentaose was synthesized according to a previously reported procedure.[1]

Synthesis of the maltopentaose-*b*-PPO, ABA triblock copolymer and 3-arm AB diblock copolymer.

AB block copolymer, ABA triblock copolymer, and 3-arm AB diblock copolymer were synthesized accordingly to the previously reported procedure.[1] The ^{1}H NMR spectra in CD_3OD are shown in **Figs. S2**, **S3**, and **S4**. The SEC chromatograms of peracetylated polymers are shown in **Fig. S5.**

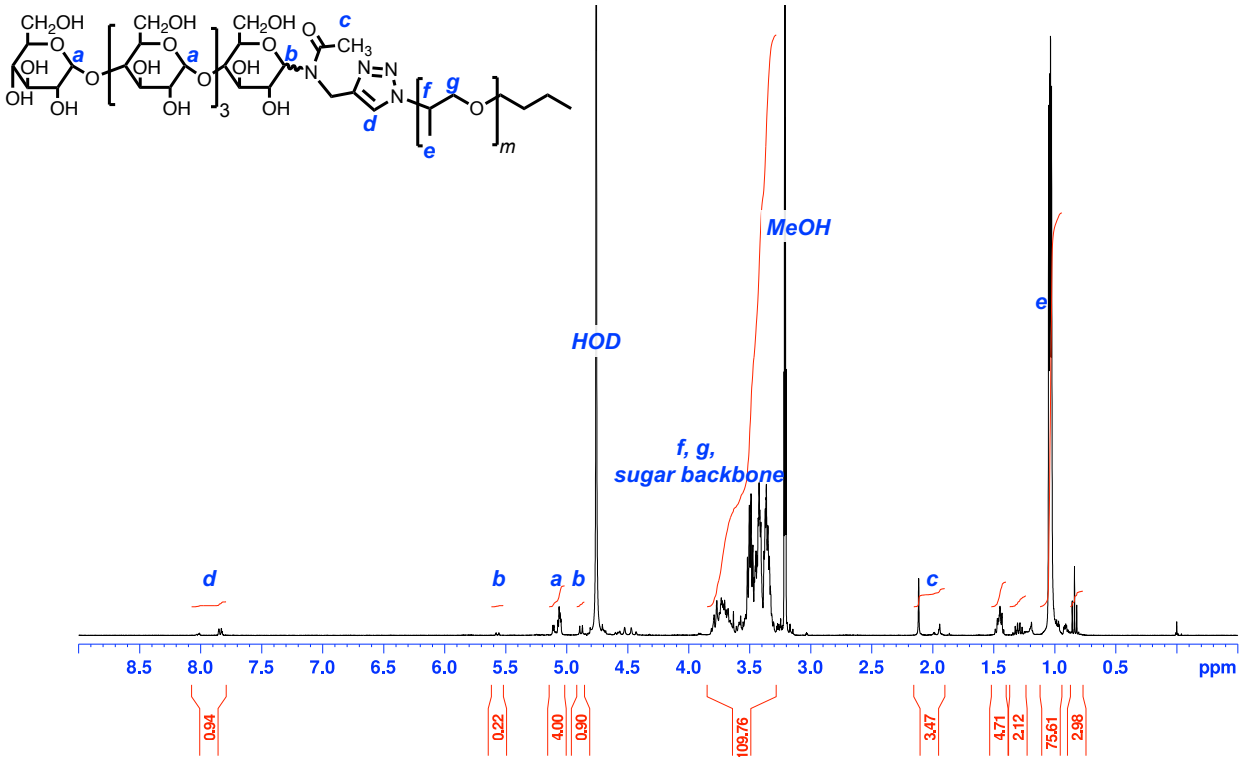

Fig. S2 ^{1}H NMR spectrum of maltopentaose-*b*-PPO in CD_3OD.

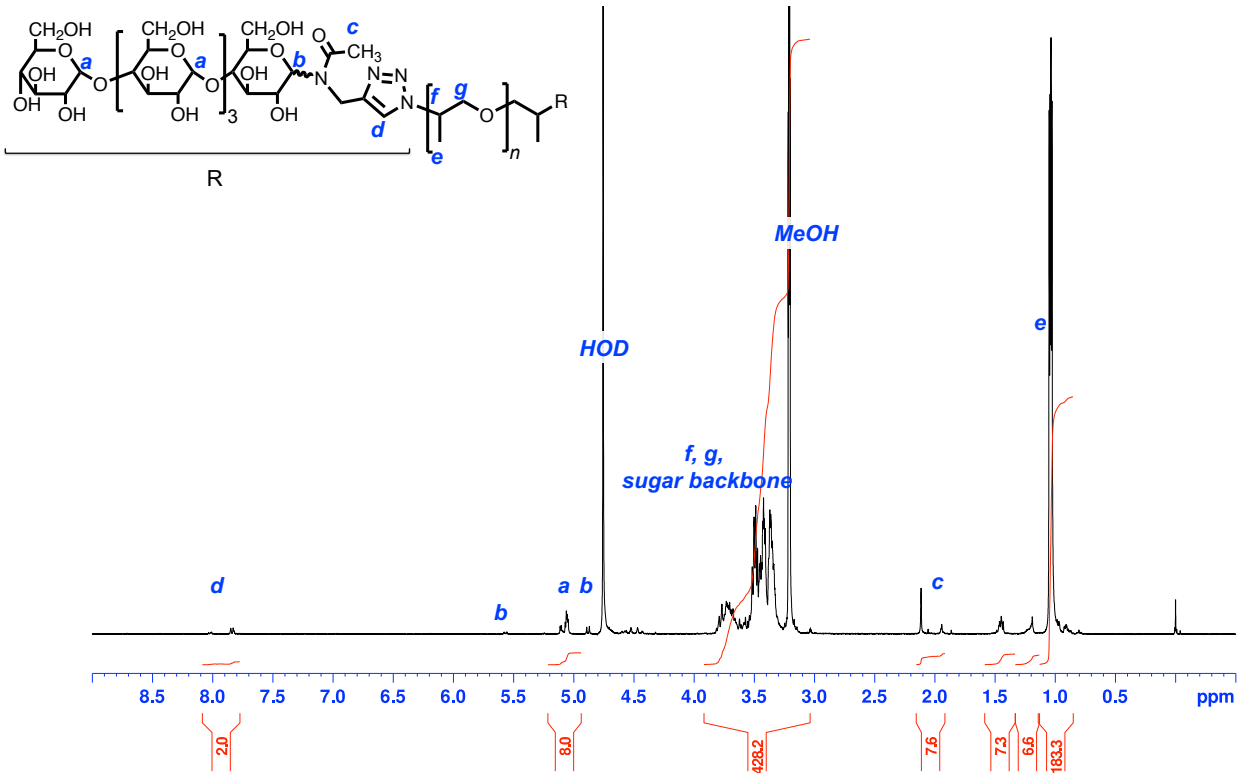

Fig. S3 ^{1}H NMR spectrum of ABA triblock copolymer in CD_3OD.

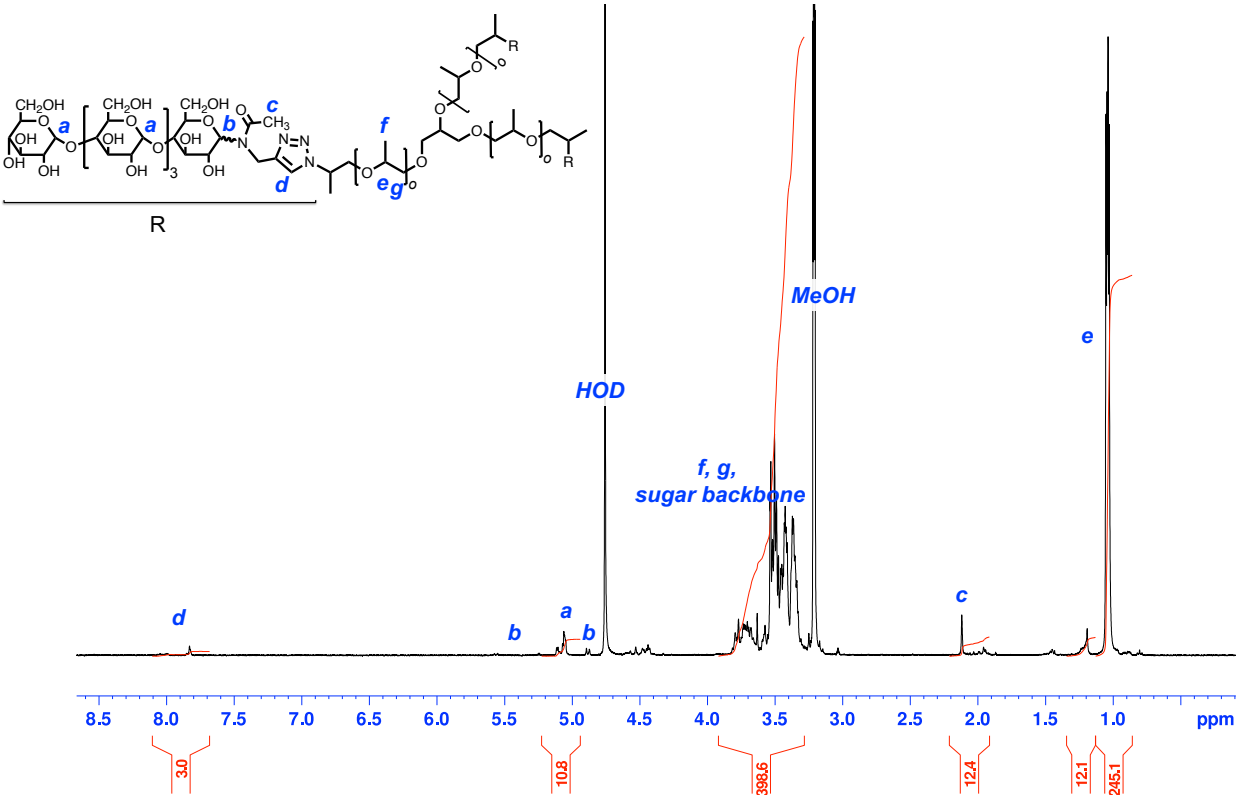

Fig. S4 ^{1}H NMR spectrum of 3-arm AB diblock copolymer in CD_3OD.

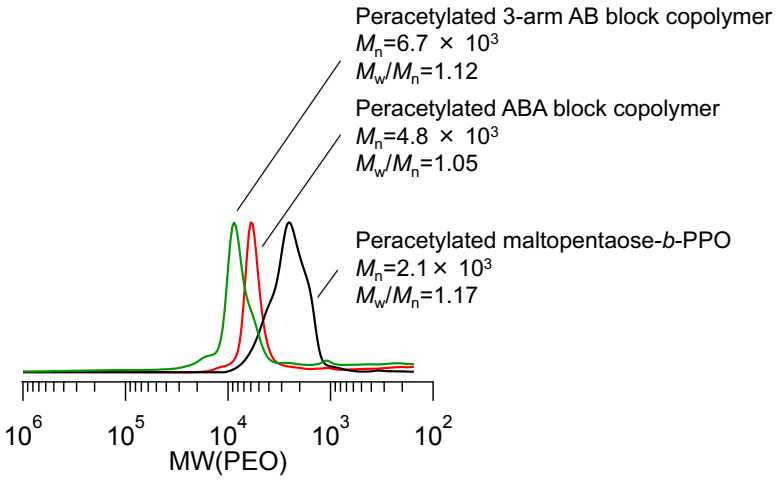

Fig. S5 SEC chromatograms of peracetylated block copolymers. It should be noted that the presence of shoulders in the peaks can be attributed to the varying elution behavior due to different degrees of acetylation.

Synthesis of the alkyne functionalized cycloamylose

cycloamylose (1.58 g, 9.73 mmol), 5-hexynoic acid (1.64 g, 14.6 mmol), DMAP (20.5 mg, 0.17 mmol), DCC (3.04 g, 14.73 mmol), and DMSO (60 mL) were added to a dry flask under an argon atmosphere, and the resulting solution was stirred for 72 h at room temperature. The crude product was purified by dialysis (regenerated cellulose membrane; Spectra/Por® 7; MWCO 1000) against DMF for 72 h and then ultrapure water for 48 h. Subsequently, the solvent was lyophilized to yield a white powder (0.996 g). The ^{1}H NMR spectrum in dimethyl sulfoxide-d_6/D_2O = 9/1 is shown in **Fig. S6**. The degree of the substitution of 5-hexynoic acid was calculated to be 25 per 100 glucose units of cycloamylose.

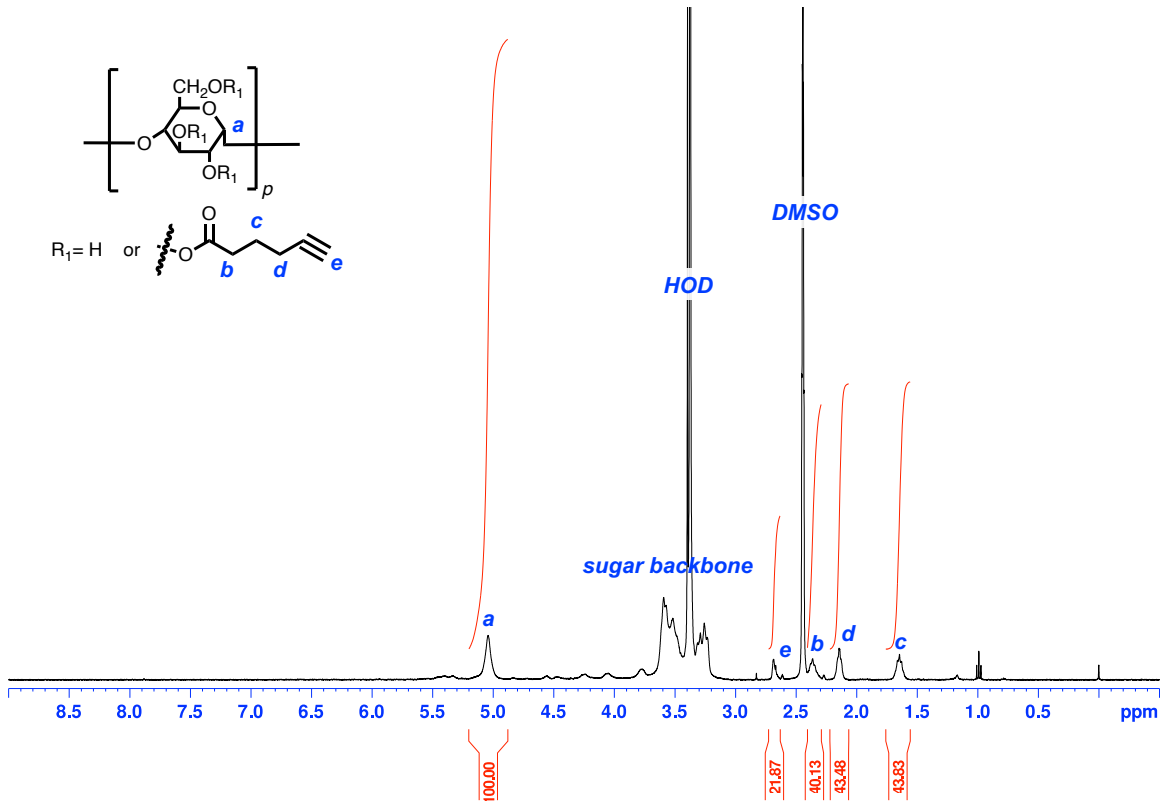

Fig. S6 ^{1}H NMR spectrum of alkyne-functionalized cycloamylose in dimethyl sulfoxide-d_6/D_2O = 9/1.

Synthesis of the azide-functionalized PPO (N_3-PPO) by anionic polymerization

N_3-PPO was synthesized by the previously reported procedure.[2] SEC (DMF; PEO): M_n (SEC) = 1.4 × 10^3 g mol^{-1}; M_n (NMR) = 1.7 × 10^3 g mol^{-1}; $Đ_M$(SEC) = 1.11. The ^{1}H NMR spectrum in chloroform-*d* is shown in **Fig. S7**, and the SEC chromatogram is shown in **Fig. S8**.

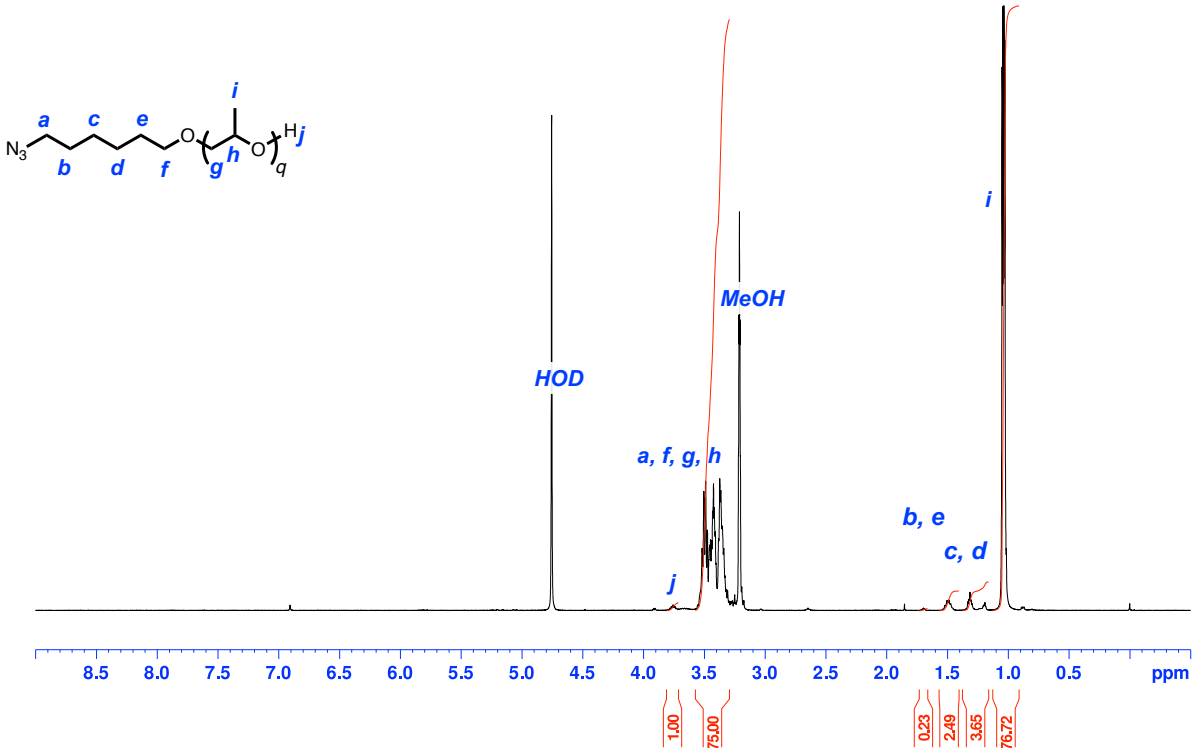

Fig. S7 ^{1}H NMR spectrum of azide-functionalized poly(propylene oxide) in chloroform-*d*.

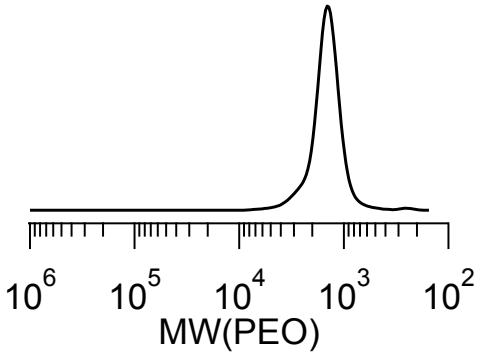

Fig. S8 SEC chromatogram of the azide-functionalized PPO.

Synthesis of the cycloamylose-*g*-PPO

A representative synthetic procedure for the synthesis of the cycloamylose-*g*-PPO with the degree of the substitution of PPO is 21 per 100 repeating units of glucose is given here. N_3-PPO (246 mg, 0.14 mmol), alkyne-functionalized cycloamylose (64 mg, 0.40 mmol), DMF (9 mL), and 1 mL of DMF solution containing CuBr (1.4 mg, 9.6 μmol) and PMDETA (17 mg, 98 μmol) were added in this order to a dry Schlenk flask under an argon atmosphere, and the mixture was stirred for 72 h at 45 °C. The crude product was purified by dialysis (regenerated cellulose membrane; Spectra/Por® 7; MWCO 3500) against DMF for 72 h, 25 mM EDTA aqueous solution for 24 h, and then ultrapure water for 24 h. Subsequently, the solvent was lyophilized to yield a white powder (0.28 g). However, unreacted N_3-PPO remained, and the crude product was again purified by dialysis (regenerated cellulose membrane; Spectra/Por® 7; MWCO 3500) against MeOH for one week. After removing the solvent, ultrapure water was added, and the solvent was lyophilized to yield a white powder (0.12 g). ^{1}H NMR spectrum in CD_3OD is shown in **Fig. S9**. The degree of the substitution of PPO is 21 per 100 glucose units of cycloamylose. The SEC chromatogram of peracetylated cycloamylose-*g*-PPO is shown in **Fig. S10**.

Acetylation of the glyco copolymers.

A representative synthetic procedure for the acetylation of glyco polymers is given here. Cycloamylose (19.9 mg), DMAP (1.60 mg, 0.020 mmol), acetic anhydride (550 μL, 5.3 mmol), and DMF (3 mL) were added in this order to a dry Schlenk flask under an argon atmosphere. The resulting solution was stirred for 24 h at 45 °C. The crude product was re-precipitated with water and then centrifuged to collect the acetylated polymer.

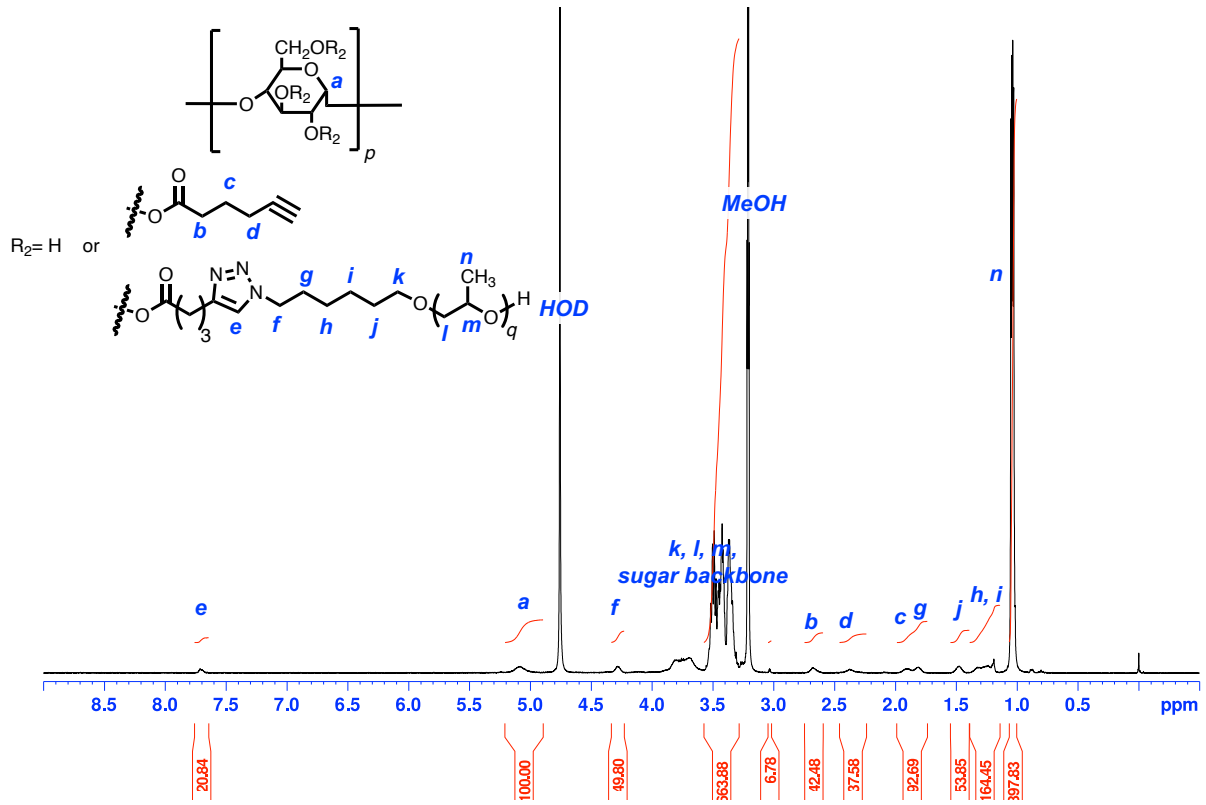

Fig. S9 ^{1}H NMR spectrum of cycloamylose-*g*-poly(propylene oxide) with the degree of the substitution of 21 PPO per 100 glucose unit of cycloamylose in CD_3OD.

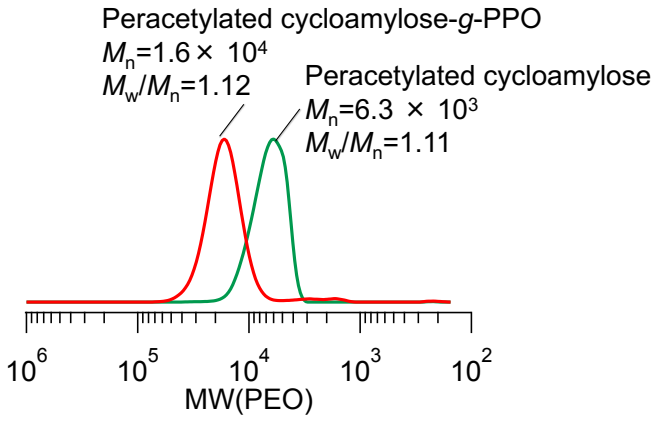

Fig. S10 SEC chromatograms of peracetylated cycloamylose-*g*-poly(propylene oxide) and peracetylated cycloamylose.

Methods

Characterization of the Polymer Assemblies

Preparation of Polymer Solutions

Ultrapure water was added to a glass vial containing the polymer powder. The resulting solutions were stirred at 0 ºC with an ice bath until the polymer was dissolved. Subsequently, the solutions were incubated at 35 °C for at least 30 minutes.

Dynamic Light Scattering (DLS)

DLS measurements were carried out using an ELSZ-2000S instrument (Otsuka Electronics Co., Ltd., Japan) operating at a wavelength of 665.2 nm and a detection angle of 165°. The obtained data were collected at 35 °C and analyzed using the unimodal method.

Fluorescence Measurements

Fluorescence spectra were recorded using a fluorescence spectrophotometer (FP-8350, JASCO, Japan) equipped with a Peltier thermostat cell holder system (ETC-115, JASCO, Japan).

Measurement conditions for the phase transition temperatures: Polymer solutions (999 μL) were added to a vial. A stock solution (1 μL) of pyrene (1.0×10^{-3} M) in ethanol was added to the vial, and the resulting solutions were incubated at room temperature for at least 15 min. The final concentration of pyrene in the vial was 1.0×10^{-6} M. Pyrene was excited at 339 nm. The slit width was set to 2.5 nm for both excitation and emission. The solutions were cooled from 40 °C to 3 °C and then were heated from 3 ºC to 40 ºC at a rate of 1 K min^{-1}.

Measurement conditions for the critical micelle concentrations: Polymer solutions (270 μL) were added to a vial. A stock solution (30 μL) of 1-anilinonaphthalene-8-sulfonic acid (1,8-ANS; 1.0×10^{-4} M) in water was added to the vial, and the resulting solutions were incubated at 35 ºC for at least 30

min. The final concentration of 1,8-ANS in the vial was 1.0×10^{-5} M. 1,8-ANS was excited at 350 nm. The slit width was set to 5.0 nm for both excitation and emission. The fluorescence spectra were recorded at 35 °C. Fluorescence intensity of 1,8-ANS was plotted as a function of logarithmic concentration of polymers. The critical micelle concentrations were calculated from the intersection of the two best-fit lines in the plot.

Transmission Electron Microscopy (TEM)

A solution of the polymers in water (5 μL; 1 mg mL^{-1}) was placed on a copper grid coated with a formvar film (PVF-C10 STEM Cu100P, Okenshoji Co., Ltd. Japan). Excess sample solution was removed using filter paper. A solution of 1 wt% phosphotungstic acid (5 μL; pH = 7.0) was added as the staining agent and then removed prior to drying the sample in a desiccator. The grid was placed in a JEM-2100 (JEOL Ltd., Japan) electron microscope, which was operated at 100 kV.

Field-flow fractionation equipped with MALS (FFF-MALS)

FFF-MALS measurements were performed using an Eclipse 3+ separation system (Wyatt Technology Europe, Dernbach, Germany) connected to a Dawn HELEOS II multiangle light scattering (MALS) detector and an Optilab rEX DSP differential refractive index (dRI) detector. An Eclipse 3 channel LC was used for the separation. The polymer solution was injected into an FFF separation channel (10 kDa regenerated cellulose membrane; 250 μm spacer M type). The cross flow was kept at 1.0- or 0-mL min^{-1} throughout the measurement time. The processing and analysis of the light scattering data and the calculation of the radius of gyration and molecular weight were performed using the software ASTRA 7. The specific refractive index increment (dn/dc) values of the polymer assemblies were determined using an Optilab rEX DSP differential refractive index (RI) detector (**Fig. S18**).

Small Angle X-ray Scattering (SAXS)

SAXS measurements were performed at the BL40B2 beamline of SPring-8 (Japan). A 25.4 × 28.9 cm^2 photon-counting detector (PILATUS3 S 2M) was placed 2.1 or 4.0 m from the sample. The wavelength (λ) of the incident X-rays was 1.0 Å. The X-ray transmittance values of the sample and of water were measured using ion chambers located in front of and behind the sample. The polymer solutions or ultrapure water were placed in a quartz capillary (diameter: 2 mm; Hilgenberg GmbH). The sample temperature was controlled using a Peltier thermostat cell holder system (TS-62, Instec, Inc., USA) and the samples were incubated at the target temperature for 10 min before the measurements. SAXS images were collected with an exposure time of 180 s. The resulting 2D SAXS images were converted into one-dimensional intensity versus q profiles by circular averaging using the FIT2D software package. The background intensity of the capillary filled with distilled water was subtracted. The scattering curves from the polymer solutions were fitted with a form factor using a bilayer vesicle model or core-shell particle models as follows.

Cross-sectional bilayer model

The form factor of the cross-sectional bilayer model can be expressed by:

$$I(q) = \frac{4\pi}{q^4}\left[(\rho_c - \rho_h)\sin\left(q\frac{t_c}{2}\right) + (\rho_h - \rho_s)\sin\left(q\frac{2t_h+t_c}{2}\right)\right]^2 \quad \text{(eq. 1)}$$

where, ρ_c, ρ_s, ρ_h, t_h, and t_c are the scattering length densities of the hydrophobic core, solvent, and hydrophilic parts and the thicknesses of the hydrophilic part and hydrophobic core, respectively. q was defined as $q = (4\pi/\lambda)\sin(\theta/2)$ (λ and θ being the wavelength and scattering angle, respectively). A Gaussian distribution of the bilayer hydrophobic thicknesses was used to take the polydispersity into account.

Core-shell particle model

The form factor of the core-shell particle model can be expressed by:

$$I(q) = \frac{1}{2}\int_0^{\pi}\{(\rho_{core} - \rho_{shell})V_c F_c(q) + (\rho_{shell} - \rho_{solvent})V_s F_s(q)\}^2 \, sin\beta d\beta \quad \text{(eq. 2)}$$

where, ρ_{core}, ρ_{shell}, $\rho_{solvent}$, V_c, V_s, and β are the electron densities of the hydrophobic core, hydrophilic shell, and solvent, the volume of the core and overall particle, and scattering vector q for averaging over the orientations, respectively.

In the case of core-shell cylinder,

$$F_c(q) = \frac{\sin(\frac{qL}{2}cos\beta)}{\frac{qL}{2}cos\beta} \times \frac{2J_1(qR_c sin\beta)}{qR_c sin\beta} \quad \text{(eq. 3)}$$

$$F_s(q) = \frac{\sin(\frac{qL}{2})cos\beta)}{(\frac{qL}{2})cos\beta} \times \frac{2J_1(qR_s sin\beta)}{q(R_s)sin\beta} \quad \text{(eq. 4)}$$

where, $J_1(x)$, L, R_s, and R_c are the first-order Bessel function of x, the length of the cylinders, the radius of the overall cylinder micelles, the radius of the inner core of the micelles, respectively. A Gaussian distribution of the thickness of the core was used to take the polydispersity into account.

In the case of core-shell sphere,

$$F_c(q) = \frac{3[sin(qr_c) - qr_c \cos(qr_c)]}{(qr_c)^3} \quad \text{(eq. 5)}$$

$$F_s(q) = \frac{3[sin(qr_s) - qr_S \cos(qr_S)]}{(qr_s)^3} \quad \text{(eq. 6)}$$

where, r_c and r_s are the radii of the core and the overall micelle, respectively. A Gaussian distribution of the thickness of the hydrophobic core was used to take the polydispersity into account.

Weakly ordered membrane stacked particle model

The scattering intensity of the weakly ordered membrane stacked particle can be described by

$$I(q) = scale \times \frac{S(q)P(q)}{q^2} + backgroud \quad \text{(eq. 7)}$$

where $S(q)$ is the structural factor of the lamellar system considering a multilayered stacking influenced thermal fluctuation based on modified Caillé theory and $P(q)$ is form factor of the individual layers. $S(q)$ can be expressed by

$$S(q) = N_{diff} + \sum_{N_K=N-2\sigma_L}^{N+2\sigma_L} S_k \qquad \text{(eq. 8)}$$

$$S_k = N_k + 2\sum_{m=1}^{N_k-1}(N_k - m)\cos(mqd)\exp\left[-\left(\frac{d}{2\pi}\right)q^2\eta\gamma\right](\pi m)^{-(d/2\pi)^2q^2\eta} \qquad \text{(eq. 9)}$$

where, N_{diff}, N, σ_L, d, γ, η are diffuse background due to the number of uncorrelated layers, total number of stacked bilayers, the gaussian polydispersity, the layer spacing, Euler constant (= 0.5772) and Caillé parameter, which is a measure for the bilayer fluctuations and depends of the bilayer rigidity, respectively. A core-shell disk model with a finite size was used for $P(q)$, which can be expressed by

$$P(q) = F(q)q^{\frac{2}{1+\exp[R_L(q-q^*)]}} \qquad \text{(eq. 10)}$$

$$F(q) = \left[(\rho_c - \rho_s)\frac{t_c\sin(qt_c)}{qt_c} + (\rho_s - \rho_0)\frac{(t_c+t_s)\sin[q(t_c+t_s)]}{q(t_c+t_s)}\right]^2 \text{(eq. 11)}$$

Eq. 10 gives dumping function to express the finite size of stacking given by q^* and R_L. ρ_c, ρ_s, ρ_0, t_c, and t_s are the electron density of the hydrophobic layer, hydrophilic layer, solvent and the half thickness of the hydrophobic layer, the thickness of the hydrophilic layer, respectively.

Table S1. Additional fitting parameters of the self-assembled cycloamylose-*g*-PPO obtained from SAXS analysis.

σ_c	d (nm)	σ_L	η	N_{diff}	q^* (nm^{-1})	R_L
0.8	9.2	1	0.25	0.01	0.001	70

Calculation of the apparent critical packing parameters of the polymer assemblies

A. spherical micelles formed by the self-assembly of the 3-arm AB diblock copolymers

1. Calculation of the volume of the PPO segment in the hydrophobic region (v)

The apparent *v* was calculated by using equation (eq. 12)

$$v = {\frac{4}{3}\pi r_{core}^3}\Big/{(N_{agg} \times N_{PPO})} \qquad \text{(eq. 13)}$$

, where r_{core}, N_{agg} and N_{PPO} is the radius of the hydrophobic core of the spherical micelles obtained from SAXS measurements (3.3 nm), the aggregation number obtained from FFF-MALS measurements (9.6) and the number of PPO segment per polymer (3), respectively. The value of *v* was calculated to be 5.2 nm^3 the polymer micelle using eq. 13. Note that the hydrophobic core of the spherical micelles contains the solvent (water), and therefore, the calculated value of *v* is larger than the actual *v* value.

2. Calculation of the area of the hydrophilic region per amphiphilic units (a)

To calculate the apparent *a*, we assumed that *a* was the surface area of the interface between the hydrophilic and hydrophobic core region of the micelle. Based on this assumption, the apparent *a* was calculated by using equation (eq. 14)

$$a = {4\pi r_{core}^2}\Big/{(N_{agg} \times N_{PPO})} \qquad \text{(eq. 14)}$$

The value of *a* can be determined to be 4.7 nm^2.

3. Calculation of the apparent critical packing parameter of the 3-arm AB diblock copolymer

The critical packing parameter (cpp) is defined as:

$$cpp = \frac{v}{a \times l} \qquad \text{(eq. 15)}$$

where *l* is the length of the hydrophobic segment. Here, the value of r_{core} (3.3 nm) was used for *l*. We therefore can determine cpp value of 3-arm AB diblock copolymer to be 0.33 using eq. 15.

B. Cylindrical micelles formed by self-assembly of the ABA triblock copolymers

1. Calculation of the volume of the PPO segment in the hydrophobic region (v)

The apparent *v* was calculated by using equation (eq. 16)

$$v = {\pi r_{core}^2 \times L_{cylinder}} \Big/ {(N_{agg} \times N_{PPO})} \quad \text{(eq. 16)}$$

, where r_{core}, $L_{cylinder}$, N_{agg}, N_{PPO} is the radius of the hydrophobic core of the cylindrical micelles obtained from SAXS analysis (3.3 nm), the half length of the cylindrical micelles (23 nm), the aggregation number obtained from FFF-MALS measurements (136), and the number of PPO segment per polymer (2), respectively. The value of *v* is therefore calculated to be 6.3 nm^3/PPO.

2. Calculation of the area of the hydrophilic region per amphiphilic units (a)

The apparent *a* was calculated by using equation (eq. 17)

$$a = {(2\pi r_{core}^2 + 2\pi r_{core} L_{cylinder})} \Big/ {(N_{agg} \times N_{PPO})} \quad \text{(eq. 17)}$$

The value of *a* can be determined to be 3.67 nm^2.

3. Calculation of the apparent critical packing parameter of the ABA triblock copolymer

Here the value of r_{core} (3.3 nm) was used for *l.* We therefore can determine cpp value of ABA triblock copolymer to be 0.47 using eq. 15.

C. Unilamellar vesicles formed by self-assembly of maltopentaose-*b*-PPO

1. Calculation of the volume of the PPO segment in the hydrophobic region (v)

The apparent *v* was calculated by using equation (eq. 18)

$$v = \left\{\frac{4}{3}\pi(r_{aq.} + t_{hydrophilic} + t_{hydrophobic})^3 - \frac{4}{3}\pi(r_{aq.} + t_{hydrophilic})^3\right\} \Big/ (N_{agg}) \quad \text{(eq. 18)}$$

, where $r_{aq.}$, $t_{hydrophilic}$, and $t_{hydrophobic}$ is the radius of the aqueous phase of the vesicles (45 nm), the thickness of the hydrophilic layer of the vesicles (2.0 nm), and the thickness of the hydrophobic layer (7.3 nm), respectively. The value of N_{agg} (3.4×10^4) was obtained from FFF-MALS measurements. Using eq. 18, the value of *v* is therefore calculated to be 7.05 nm^3/PPO.

2. Calculation of the area of the hydrophilic region per amphiphilic units (a)

The apparent *a* was calculated by using equation (eq. 19)

$$a = \{4\pi(r_{all} - t_{hydrophilic})^2 + 4\pi(r_{aq.} + t_{hydrophilic})^2\} \Big/ (N_{agg}) \quad \text{(eq. 19)}$$

, where r_{all} is the radius of the vesicles obtained from DLS analysis (55 nm).

The value of *a* can be determined to be 1.84 nm^2 using eq. 19.

3. Calculation of the apparent critical packing parameter of maltopentaose-*b*-PPO

Here the value of r_{core} (7.3/2 nm = 3.65 nm) was used for *l*. We therefore can determine cpp value of maltopentaose-*b*-PPO to be 1.05 using eq. 15.

D. Multilamellar vesicles formed by self-assembly of cycloamylose-*g*-PPO

Here, we assumed that the multilamellar vesicles consist of four bilayer membranes based on the SAXS analysis. Since the sum of the aggregation numbers of each layer is equal to the total aggregation numbers obtained from FFF-MALS ($N_{agg} = 6.6 \times 10^3$), it can be expressed by:

$$N_{1\,agg} + N_{2\,agg} + N_{3\,agg} + N_{4\,agg} = 6.6 \times 10^3 \qquad \text{(eq. 20)}$$

where, $N_{1\,agg}$, $N_{2\,agg}$, $N_{3\,agg}$, and $N_{4\,agg}$ are the aggregation number of first, second, third, and fourth bilayer vesicle, respectively. The volume of vesicles (v) and the number of aggregations is correlated and can be expressed by the following relationship.

$$v = kN_{agg} \quad \text{(eq. 21)}$$

where, k is a proportional constant. Threfore, the volume, the number of vesicles in each layer, and the aggregation numbers can be expressed as follows.

$$\frac{v_2}{v_1} = \frac{N_{2\,agg}}{N_{1\,agg}}, \qquad \frac{v_3}{v_1} = \frac{N_{3\,agg}}{N_{1\,agg}}, \qquad \frac{v_4}{v_1} = \frac{N_{4\,agg}}{N_{1\,agg}} \qquad \text{(eq. 22)}$$

The distance from the center of the vesicle to each inner water layer is defined as r_1, r_2, r_3, and r_4 respectively, the volume of the vesicle in each layer can be expressed as follows

$$v_1 = \frac{4}{3}\pi\{(r_{all})^3 - (r_1)^3\} \qquad \text{(eq. 23)}$$

$$v_2 = \frac{4}{3}\pi\{(r_1)^3 - (r_2)^3\} \qquad \text{(eq. 24)}$$

$$v_3 = \frac{4}{3}\pi\{(r_2)^3 - (r_3)^3\} \qquad \text{(eq. 25)}$$

$$v_4 = \frac{4}{3}\pi\{(r_3)^3 - (r_4)^3\} \qquad \text{(eq. 26)}$$

, where r_{all} is the radius of the multilamellar vesicles obtained from SAXS analysis (49 nm). Since $r_1, r_2, r_3, and\ r_4$ are 39.8 nm, 30.6 nm, 21.4 nm, and 12.2 nm, respectively. Thus, $v_{1,} v_2, v_3$, and v_4 can be calculated to be 2.3×10^5 nm^3, 1.4×10^5 nm^3, 7.9×10^4

nm^3, and $3.3 \times 10^4 nm^3$, respectively. Therefore, using eq. 20 and eq. 22, the aggregation numbers of each vesicle is calculated to be $N_{1\,agg} = 3.11 \times 10^3, N_{2\,agg} = 1.96 \times 10^3, N_{3\,agg} = 1.07 \times 10^3, and\ N_{4\,agg} = 4.5 \times 10^2$.

1. Calculation of the volume of the PPO segment in the hydrophobic region (v)

The apparent v_1 was calculated by using equation (eq. 27)

$$v_1 = \left\{\frac{4}{3}\pi(r_1 + t_{hydrophilic} + t_{hydrophobic})^3 - \frac{4}{3}\pi(r_1 + t_{hydrophilic})^3\right\} \Big/ (N_{1\,agg} \times N_{PPO}) \quad \text{(eq. 27)}$$

, where v_1, r_1, $t_{hydrophilic}$, and $t_{hydrophobic}$ is the volume of the PPO segment in the most outer hydrophobic region, the radius from the center of the multilamellar vesicle to the most outer inner aqueous phase, the thickness of the hydrophilic layer of the multilamellar vesicles (2.2 nm), and the thickness of the hydrophobic layer (4.8 nm), respectively. The value of $N_{1\,agg}$ (3.18×10^3) was obtained the previous calculation. N_{PPO} can be calculated to be $N_{PPO} = \frac{number\ averaged\ molecular\ weight\ of\ polymer}{moleuclar\ weight\ of\ the\ repeating\ unit} \times DS\ of\ PPO = \frac{4.2 \times 10^3}{162} \times \frac{21}{100} = 5.5$. Using eq. 27, we were able to calculate the value of *v* (7.0 nm^3/PPO).

2. Calculation of the area of the hydrophilic region per amphiphilic units (a)

The apparent a_1 was calculated by using equation (eq. 28)

$$a_1 = \{4\pi(r_{all} - t_{hydrophilic})^2 + 4\pi(r_1 + t_{hydrophilic})^2 \Big/ (N_{1\,agg} \times N_{PPO}) \quad \text{(eq. 28)}$$

, where r_{all} is the radius of the vesicles obtained from SAXS analysis (49 nm).

The value of *a* can be determined to be 2.9 nm^2 using eq. 28.

3. Calculation of the apparent critical packing parameter of cycloamylose-g-PPO

Here, the value of r_{core} (2.4 nm) was used for *l*. We therefore can determine cpp value of cycloamylose-

g-PPO to be 0.99 using eq. 15.

Complex formation of triiodide ion with the glyco polymers

Standard iodine-iodide solution (5 g of KI, 0.2 g of I_2 in 250 ml; 40 µl) and polymer solution (40 µl, 1, 5, or 10 mg mL^{-1}) were mixed and diluted with water to 4.0 ml. The absorption spectra of these solutions were recorded on a UV-vis spectrophotometer (V-750, JASCO) with a Peltier thermostat cell holder system to scan the 300−800 nm wavelength range. Samples were analyzed in a 1 cm quartz cuvette at 25 ºC.

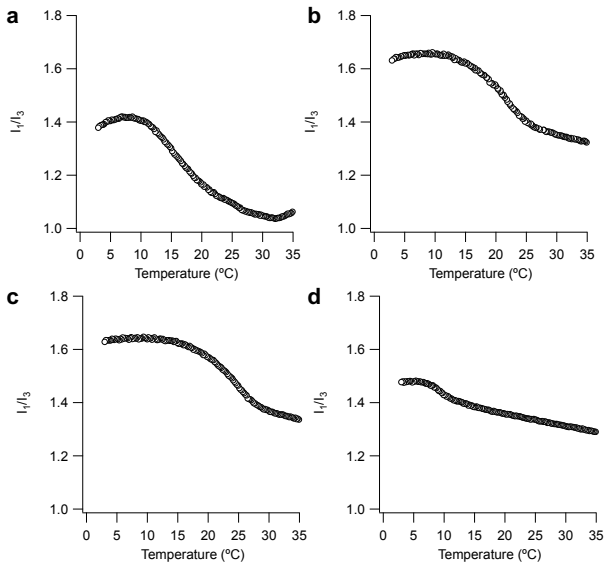

Fig. S11 Plots of the I_1/I_3 ratio of pyrene in the presence of (a) AB diblock copolymer, (b) ABA triblock copolymer, (c) 3-arm AB diblock copolymer, (d) cycloamylose-*g*-PPO in water upon cooling of the solutions. Concentrations: [Polymer] = 1.0 mg mL^{-1}, [pyrene] = 1×10^{-6} M. Cooling rate = 1 K min^{-1}.

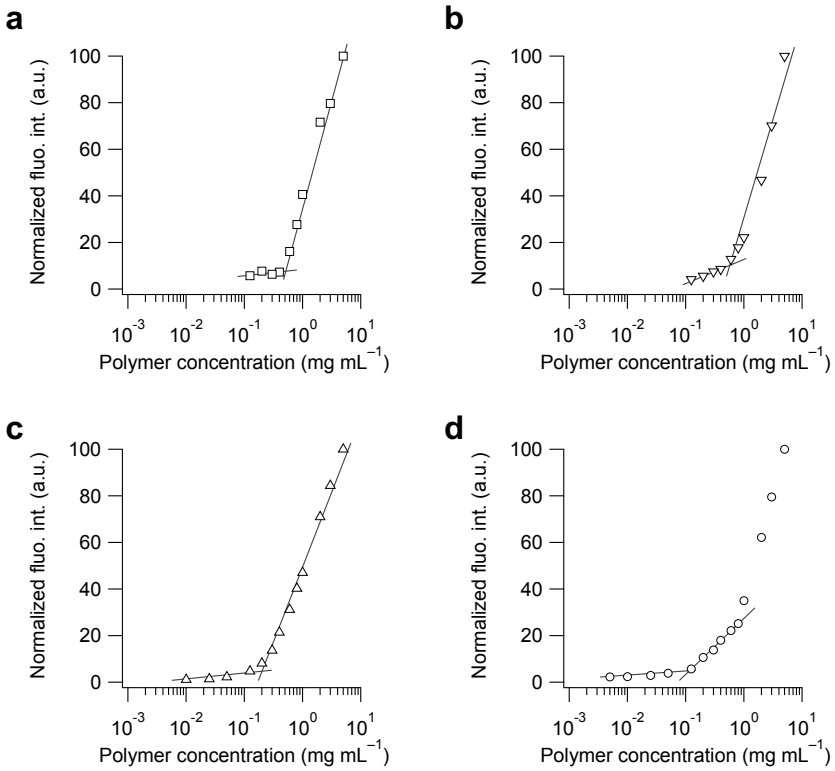

Fig. S12 The normalized fluorescence intensity of 1,8-ANS in water at 35 ºC at 470 nm plotted against the polymer concentration of a) AB block copolymer, b) ABA block copolymer, c) 3-arm AB block copolymer, and d) cyclic graft copolymer; [1,8-ANS] = 1.0×10^{-5} M.

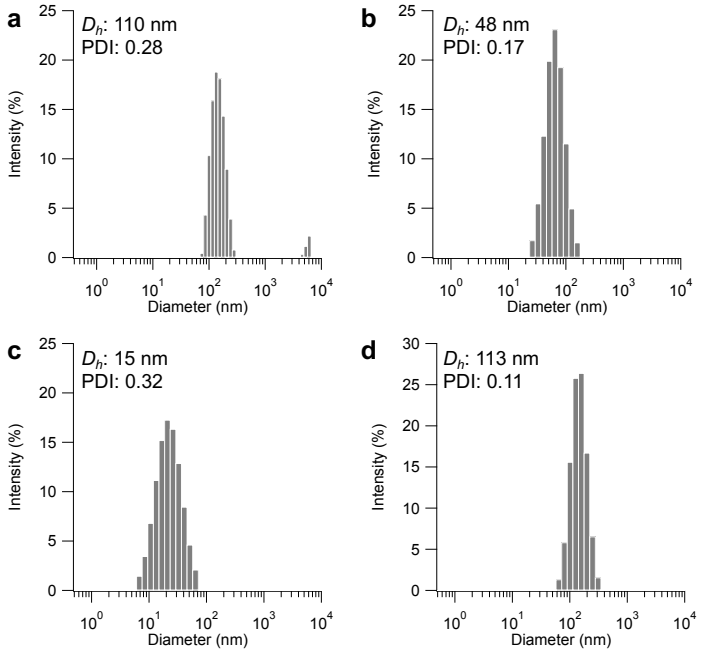

Fig. S13 Size distribution of self-assembled particles of (a) AB diblock copolymer, (b) ABA triblock copolymer, (c) 3-arm AB diblock copolymer, (d) cycloamylose-*g*-PPO solution.

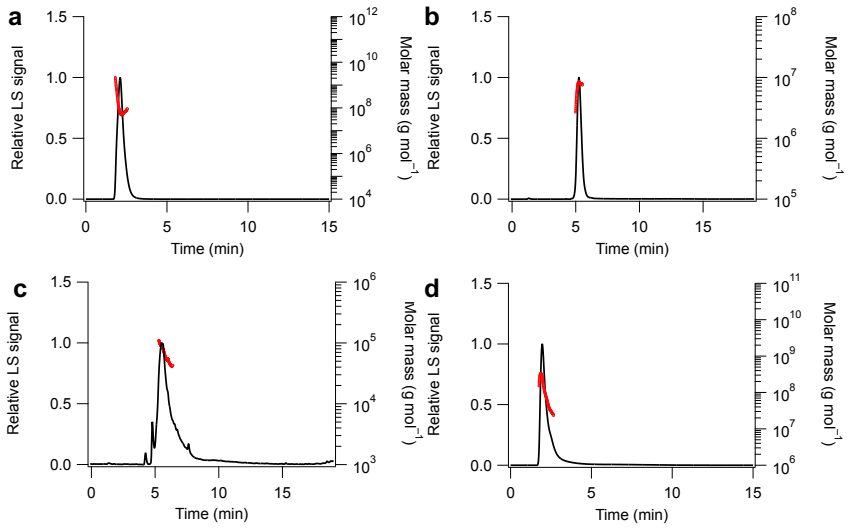

Fig. S14 The FFF-fractograms of (a) AB diblock copolymer, (b) ABA triblock copolymer, (c) 3-arm AB diblock copolymer, (d) cycloamylose-*g*-PPO solution: 90º light scattering signal (black solid line) and the molar mass (red solid line).

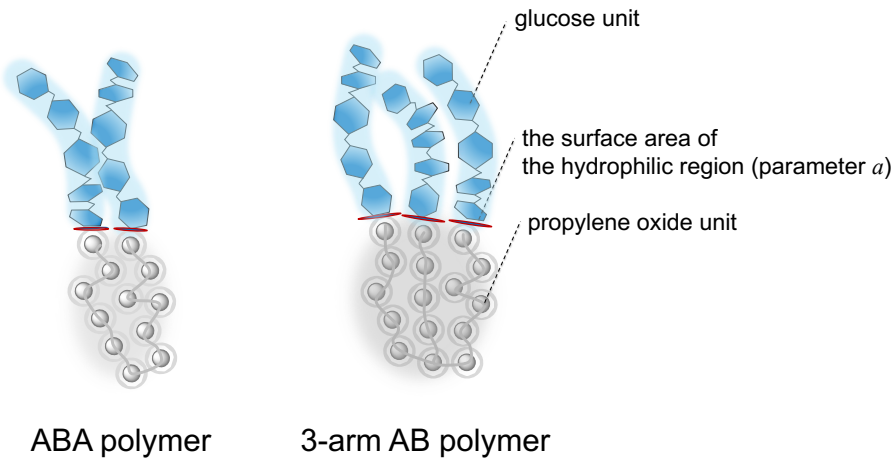

Fig. S15. Schematic illustration of the proposed polymer chain folding of ABA triblock copolymer (left) and 3-arm AB diblock copolymer (right). In the star polymers, when they gather around the branching point of PPO, PPO chains are not able to assemble closely together. The surface area of the hydrophilic region is therefore larger than in the ABA polymers. The illustrations do not draw to scale.

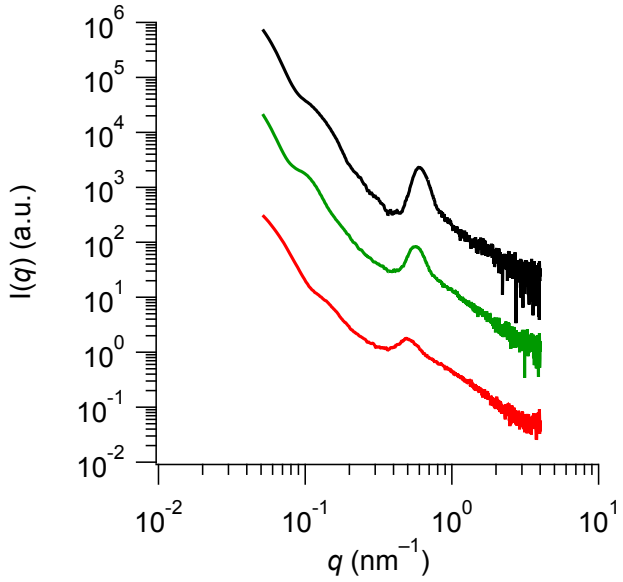

Fig. S16 SAXS profiles of a solution of cycloamylose-*g*-PPO with the degree of the substitution of 11 PPO groups per 100 glucose units of cycloamylose (black line), with the degree of the substitution of 9 PPO groups per 100 glucose units of cycloamylose (green line), and with the degree of the substitution of 6 PPO groups per 100 glucose units of cycloamylose (red line). Concentration: [polymers] = 1.0 mg mL^{-1}.

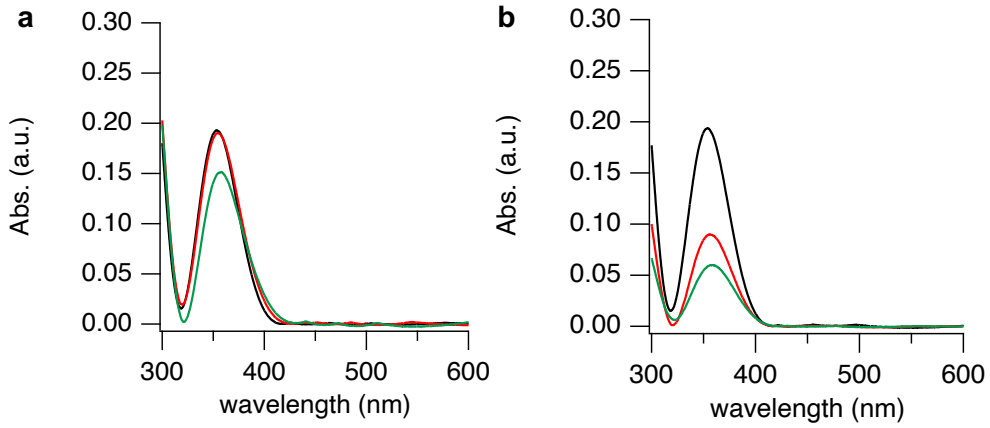

Fig. S17 UV-vis spectra of potassium iodide and iodine solutions in the presence of cycloamylose-*g*-PPO at the concentration of 0.25 μg mL^{-1} (black line), 1.25 μg mL^{-1} (red line), and 2.5 μg mL^{-1} (green line) and (b) alkyne-functionalized cycloamylose at the concentration of 0.25 μg mL^{-1} (black line), 1.25 μg mL^{-1} (red line), and 2.5 μg mL^{-1} (green line). Concentrations: [KI] = 0.2 mg mL^{-1}, [I_2] = 0.25 μg mL^{-1}.

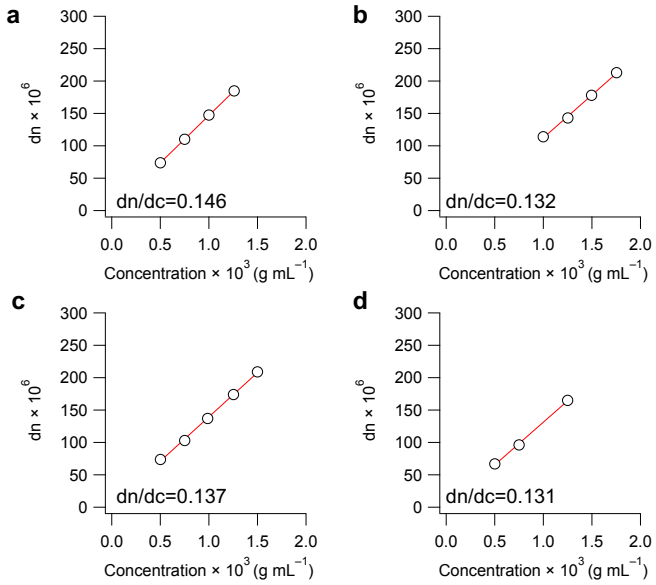

Fig. S18 Concentration dependence of refractive index increment for (a) AB diblock copolymer, (b) ABA triblock copolymer, (c) 3-arm AB diblock, (d) cycloamylose-*g*-PPO.

Additional references

[1] T. Nishimura, Y. Sasaki, K. Akiyoshi, *Adv. Mater.* **2017**, *29*, 1702406.

[2] T. Nishimura, S. Shishi, Y. Sasaki, K. Akiyoshi, *J. Am. Chem. Soc.* **2020**, *142*, 11784-11790.